

# ChemComm

Accepted Manuscript



This is an *Accepted Manuscript*, which has been through the Royal Society of Chemistry peer review process and has been accepted for publication.

*Accepted Manuscripts* are published online shortly after acceptance, before technical editing, formatting and proof reading. Using this free service, authors can make their results available to the community, in citable form, before we publish the edited article. We will replace this *Accepted Manuscript* with the edited and formatted *Advance Article* as soon as it is available.

You can find more information about *Accepted Manuscripts* in the [Information for Authors](#).

Please note that technical editing may introduce minor changes to the text and/or graphics, which may alter content. The journal's standard [Terms & Conditions](#) and the [Ethical guidelines](#) still apply. In no event shall the Royal Society of Chemistry be held responsible for any errors or omissions in this *Accepted Manuscript* or any consequences arising from the use of any information it contains.

Cite this: DOI: 10.1039/c0xx00000x

www.rsc.org/xxxxxx

ARTICLE TYPE

# Functionalization of Robust Zr(IV)-based Metal-Organic Framework Films via Postsynthetic Ligand Exchange†

Honghan Fei,<sup>a</sup> Sonja Pullen,<sup>b</sup> Andreas Wagner,<sup>b</sup> Sascha Ott,<sup>b,\*</sup> and Seth M. Cohen<sup>a,\*</sup>

Received (in XXX, XXX) Xth XXXXXXXXX 20XX, Accepted Xth XXXXXXXXX 20XX

DOI: 10.1039/b000000x

**A facile and efficient fabrication approach for homogeneous, crack-free UiO-66 films with exceptionally high crystallinity and tunable thickness on a transparent and conductive glass substrate is reported. Two functionalized species, a catechol ligand and a Fe<sub>2</sub> complex with structural resemblance to the active site of [FeFe] hydrogenase, were introduced into the MOF films by postsynthetic exchange. Voltammetric studies show the [FeFe] complex in the thinner UiO-66 films (2-5 μm) can be reduced electrochemically.**

Metal-organic frameworks (MOFs) are crystalline materials with exceptionally high surface area and porosity<sup>1</sup> that have gathered extensive attention for applications in gas absorption,<sup>2,3</sup> catalysis,<sup>4</sup> and molecular separation/sensing.<sup>5,6</sup> In recent years, many efforts were directed towards the growth of MOF films,<sup>7</sup> which is important for utilizing MOF materials<sup>8</sup> in functional electronic devices.<sup>9</sup> Most of these technological applications require chemically “inert” MOFs that are robust under harsh chemical conditions.<sup>10</sup> Except some limited studies on MIL-53(Al)<sup>11</sup> and MIL-101(Cr)<sup>12</sup>, functionalized robust MOFs have not been widely described in the realm of thin film MOF growth.<sup>7,13,14</sup>

Unlike zeolites and other porous materials, the organic components in MOFs allow for the introduction of a wide variety of functional groups through either direct synthesis<sup>15</sup> or postsynthetic approaches.<sup>16</sup> Compared with other functionalization methods, postsynthetic ligand exchange (PSE, also termed “SALE”, solvent-assisted ligand exchange) has been increasingly studied as a facile and efficient functionalization approach in robust MOFs.<sup>17,18</sup> Compared with extensive studies on postsynthetic functionalization of bulk MOF materials, only a few examples of postsynthetic covalent modification (PSM) have been described on MOF thin films.<sup>19-22</sup> Importantly, the synthetic conditions described for MOF films may preclude installation of different functionalities using a direct synthetic approach. For example, reports of using 2-amino-1,4-benzenedicarboxylic acid (NH<sub>2</sub>-bdc) posed difficulties in preparing a high-quality, amino-functionalized Cu-paddlewheel SURMOF (surface-mounted MOFs) films that had been readily obtained with naphthalenedicarboxylic acid.<sup>7,21</sup>

Herein, we report a facile and efficient method to fabricate robust Zr(IV)-based UiO-66 (UiO = University of Oslo) films with adjustable thickness on fluoride-doped tin oxide (FTO) glass

substrates via solvothermal growth. The resultant uniform and crack-free films strongly adhere to the substrate and exhibit high stability comparable to bulk UiO-66. More importantly, this study is a rare example of PSE for the functionalization of MOF films. An open metal-binding functionality (catechol group) and a thermally labile Fe<sub>2</sub> complex, reminiscent of the [FeFe] hydrogenase active site, were successfully incorporated into UiO-66 films.

UiO-66 films were solvothermally grown on an FTO substrate via a method similar to recently reported studies.<sup>23-25</sup> FTO was chosen as a transparent and conducting glass substrate, and was pretreated with an aqueous 1 mM 1,4-benzenedicarboxylic acid (H<sub>2</sub>bdc) solution to generate a self-assembled monolayer (SAM) of carboxylic acid-terminated organic ligands. The H<sub>2</sub>bdc concentration for the pretreatment was found to be important to produce optimal films as higher concentrations (5-10 mM) lead to thicker MOF films with weaker film adhesion to the substrate. The SAM-decorated FTO was introduced to a DMF solution containing ZrCl<sub>4</sub>, H<sub>2</sub>bdc, and benzoic acid with a molar ratio of 1:1:60, which was heated to 120 °C for 24 h. It was found that the film thickness can be decreased by lowering the concentration of H<sub>2</sub>bdc during synthesis (e.g. ratio of 1:0.6:60). The large excess of benzoic acid as a modulator was found to be necessary to control crystal growth on the FTO glass.

The MOF films are homogeneous and crack-free throughout the FTO glass substrate with sizes from 0.5~2 cm<sup>2</sup>. The top-view field-emission scanning electron microscope (FE-SEM) images showed the MOF films were stacked in compact arrays with crystalline particles over a long range, and exhibited monodisperse UiO-66 microcrystals with an octahedral morphology and particle size of ~2 μm or ~0.5 μm for thicker or thinner films, respectively (Figure 1 and Figure S1-S2). A cross-sectional SEM image indicates that the films consist of layers of MOF particles. The total thickness of the films obtained from a 1:1 ratio of ZrCl<sub>4</sub> and H<sub>2</sub>bdc were ~20 μm. Thinner films made with less H<sub>2</sub>bdc were of a thickness of 2-5 μm and showed less uniform substrate coverage. The composition and crystallinity of the MOF films was further confirmed with powder X-ray diffraction (PXRD), indicating a phase-pure UiO-66 topology (Figure 2, Figure 3, and Figure S3). Importantly, both the thicker and the thinner UiO-66 films were stable in water (including treatment with dilute HCl, pH=3) and a variety of organic solvents (MeOH, CHCl<sub>3</sub>, CH<sub>3</sub>CN, etc.).

Recently, PSE has been employed as an efficient tool to

functionalize MOFs under mild conditions.<sup>26</sup> The use of this methodology for MOF-films has however been highly limited to date. To the best of our knowledge, there is only one report of a MOF film (based on a more labile Zn-paddlewheel secondary building unit) to undergo PSE and, in this example, PSE was confined to the external surface of the film.<sup>20</sup> Herein, we demonstrate that the UiO-66 films allow for the PSE with two different functional groups, which cannot be directly incorporated during solvothermal film growth.

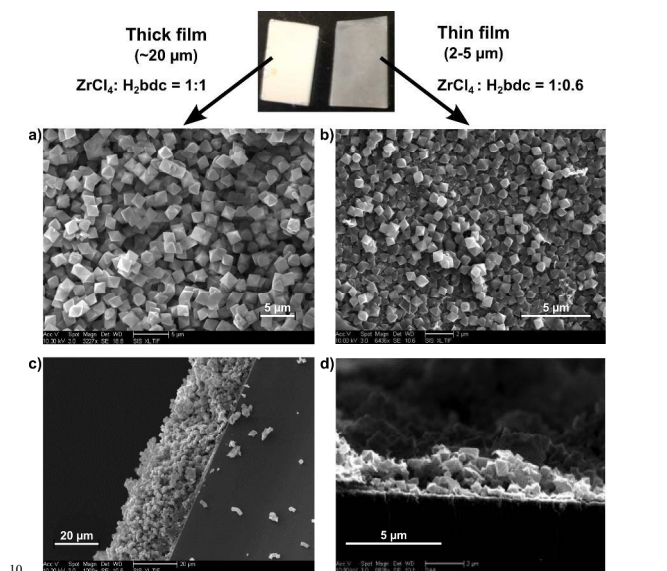


**Fig. 1** Film morphologies: Top-view SEM image of a) thicker (~20 μm) and b) thinner (~2-5 μm) UiO-66 film. Cross-sectional SEM image of c) thicker and d) thinner films.

In an initial proof-of-concept study, a catechol ligand was introduced into the 20 μm UiO-66 film by PSE as an approach to incorporate open metal-chelating groups onto MOF films (Figure 2). PSE was carried out by carefully placing a UiO-66 film into a dilute, neutral (pH=7) aqueous solution containing 2,3-dihydroxy-1,4-benzenedicarboxylic acid (H<sub>2</sub>catbdc). Incubation for 24 h at room temperature was followed by washing of the film with water, water/ethanol (v/v=1:1), and ethanol. The resulting UiO-66-CAT film was uniform, off-white in colour, and strongly adhered to the substrate (Figure 2). PXRD of the treated MOF film confirmed the high phase purity of UiO-66-CAT. Top-view SEM images showed no apparent change in microcrystalline particle size, but a slight decrease in crystallinity after PSE (Figure S4). The degree of H<sub>2</sub>catbdc functionalization in UiO-66-CAT film was ~63% as determined by <sup>1</sup>H NMR of HF/d<sup>6</sup>-DMSO digested films (Figure S5). The degree of functionality is thus significantly higher than achieved with the bulk MOF (~28%) under identical PSE conditions (room temperature for 24 h, see Table S1).<sup>27</sup>

The highly robust UiO-66-CAT films with open metal-chelating sites allowed for efficient metalation to introduce an accessible metal centre into the MOF material. Treatment of UiO-66-CAT films with FeCl<sub>3</sub> in aqueous solution results in films with a brown colour, indicative of formation of the Fe-catecholato species. The film remains highly uniform, and both PXRD and SEM confirm the preservation of phase purity and

identical particle morphology, respectively (Figure 2, Figure S6). EDX indicated an atomic ratio of 1:0.16 (Zr:Fe), confirming ~26% of catechol sites were metalated with Fe (Figure S7).

Having established a viable procedure for PSE in UiO-66 films on FTO, attempts were made to introduce a known proton reduction catalyst with structural features of the [FeFe] hydrogenase active site into films of different thickness. PSE was carried out by placing UiO-66 films in an aqueous solution of 20 mM [FeFe](dcbdt)(CO)<sub>6</sub> (dcbdt=2,3-dithiolato-1,4-benzene dicarboxylic acid, Figure 3) at room temperature for 24-72 h, followed by extensive washing with MeOH, and drying in air.<sup>28</sup> The treated MOF (UiO-66-[FeFe](dcbdt)(CO)<sub>6</sub>) films remain homogenous and crack-free, and exhibit particles with an identical size (~2 μm or 0.5-1 μm) and shape as the UiO-66 films prior to PSE as evidenced by top-view SEM (Figure 4).

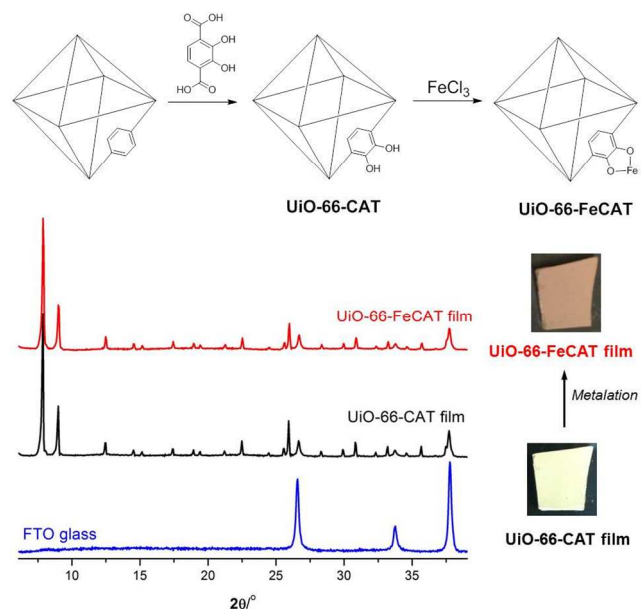


**Fig. 2** Top: synthesis of UiO-66-CAT film and UiO-66-FeCAT film. Bottom left: PXRD of bare FTO glass (blue), UiO-66-CAT film on FTO glass (black), and UiO-66-FeCAT film on FTO glass (red). Bottom right: Photograph of UiO-66-CAT film and UiO-66-FeCAT film on a FTO substrate (~0.8 cm<sup>2</sup>).

The phase purity of the UiO-66-[FeFe](dcbdt)(CO)<sub>6</sub> films was confirmed with PXRD, demonstrating a highly crystalline UiO-66 structure (Figure 3, Figure S3). Diffuse reflectance UV-Vis spectroscopy of post-exchanged films confirmed the incorporation of [FeFe](dcbdt)(CO)<sub>6</sub> with its characteristic absorption at 350 nm (Figure S8). The orange-yellow colour of the films after PSE is even visible to the eye (Figure 3, Figure S3). The MOF particles could be liberated from the FTO substrate via sonication, which allowed for additional characterization of the material. FTIR of UiO-66-[FeFe](dcbdt)(CO)<sub>6</sub> particles removed from FTO showed three bands at 2078 cm<sup>-1</sup>, 2038 cm<sup>-1</sup>, and 2001 cm<sup>-1</sup>, characteristic of the CO stretch of the [FeFe] complex (Figure S9). The degree of [FeFe] functionality was found to be between ~32-35% for both film thicknesses, as evidenced by energy-dispersed X-ray spectroscopy (EDX) and/or C/H/N/S combustion analysis (Figure

S10, Table S2). Similar to  $\text{H}_2\text{catbdc}$ , the incorporation of  $[\text{FeFe}](\text{dcbdt})(\text{CO})_6$  into the UiO-66 film is also increased when compared to previous studies on bulk UiO-66 (~14% incorporation),<sup>28</sup> which is likely due to an expanded liquid-solid interface. Generally, the procedures we have used when performing PSE on bulk UiO-66, the powdered solid is not stirred in order to reduce damage to the particles. The lack of stirring likely limits particle exposure to the solution; therefore, when formulated into the films described here, the particle-solution interface should be increased substantially. Particle size does not seem to contribute to the different rates of PSE, as MOF crystal sizes in the bulk (~200-500 nm) are comparable to those in the thinner UiO-66 films used for PSE here.

Control experiments performed with  $[\text{FeFe}](\text{bdt})(\text{CO})_6$  (bdt = benzene-1,2-dithiolate), which has the same metal cluster, but lacks the coordinating carboxylates on the dithiolate ligand, support that incorporation of  $[\text{FeFe}](\text{dcbdt})(\text{CO})_6$  occurred via a PSE process. Exposing the UiO-66 film to identical PSE conditions using  $[\text{FeFe}](\text{bdt})(\text{CO})_6$  showed no substantial incorporation of  $[\text{FeFe}](\text{bdt})(\text{CO})_6$  after rinsing with MeOH. The lack of colour change of the film and absence of CO bands in the FTIR spectrum (Figure S9) confirm that this complex was not incorporated into the material. This negative control supports our contention that  $[\text{FeFe}](\text{dcbdt})(\text{CO})_6$  is incorporated into the UiO-66 films via a PSE process and not simply encapsulated within the MOF pores.

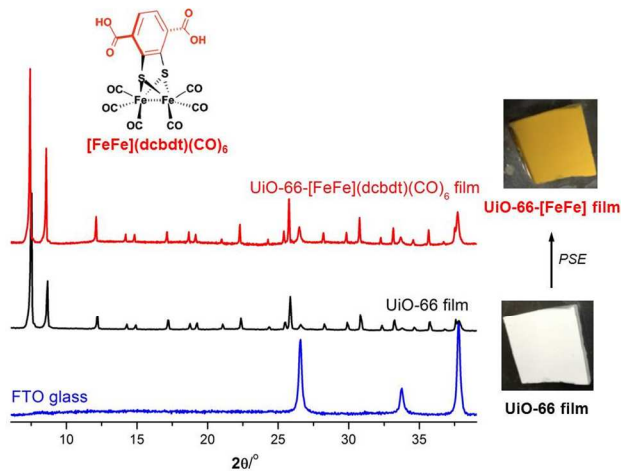


**Fig. 3** Left: PXRD of bare FTO glass (blue), thicker UiO-66 film on FTO glass (black), and corresponding UiO-66-[FeFe](dcbdt)(CO)<sub>6</sub> film on FTO glass (red). Right: photographs of thicker (~20 μm) UiO-66 and UiO-66-[FeFe](dcbdt)(CO)<sub>6</sub> films on a FTO substrate (~1 cm<sup>2</sup>).

Control experiments performed with  $[\text{FeFe}](\text{bdt})(\text{CO})_6$  (bdt = benzene-1,2-dithiolate), which has the same metal cluster, but lacks the coordinating carboxylates on the dithiolate ligand, support that incorporation of  $[\text{FeFe}](\text{dcbdt})(\text{CO})_6$  occurred via a PSE process. Exposing the UiO-66 film to identical PSE conditions using  $[\text{FeFe}](\text{bdt})(\text{CO})_6$  showed no substantial incorporation of  $[\text{FeFe}](\text{bdt})(\text{CO})_6$  after rinsing with MeOH. The lack of colour change of the film and absence of CO bands in the FTIR spectrum (Figure S9) confirm that this complex was not incorporated into the material. This negative control supports our contention that  $[\text{FeFe}](\text{dcbdt})(\text{CO})_6$  is incorporated into the UiO-

66 films via a PSE process and not simply encapsulated within the MOF pores.

The electrochemical behaviour of UiO-66-[FeFe](dcbdt)(CO)<sub>6</sub> was investigated by cyclic voltammetry (CV). In homogenous DMF solution,  $\text{Fe}_2(\text{dcbdt})(\text{CO})_6$  exhibits a quasi-reversible two-electron reduction at  $E_{1/2} = -1.18$  V vs.  $\text{Ag}/\text{Ag}^+$  ( $E_{1/2} = (E_{\text{pa}} - E_{\text{pc}})/2$ ; Figure 5), thus at a similar potential as that of previously reported  $\text{Fe}_2(\text{bdt})(\text{CO})_6$ .<sup>29</sup> The relatively large difference between cathodic and anodic peak potentials in the CV of  $[\text{FeFe}](\text{dcbdt})(\text{CO})_6$  is not yet fully understood, but presumably caused by processes that involve the COOH groups.

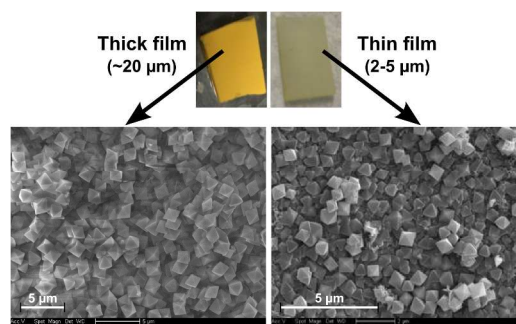


**Fig. 4** Left: Top: Photographs of thick and thin films after PSE. Bottom left: Top-view SEM image of thicker (20 μm) UiO-66-[FeFe](dcbdt)(CO)<sub>6</sub> film. Bottom-right: Top-view SEM image of thinner (2-5 μm) UiO-66-[FeFe](dcbdt)(CO)<sub>6</sub> film.

The UiO-66-[FeFe](dcbdt)(CO)<sub>6</sub> films show a varying electrochemical response that depends on the thickness of the film (Figure 5). CVs of thinner films (2-5 μm) show cathodic and anodic feature at -1.45 V and -0.8 V, respectively, giving rise to a formal  $E_{1/2} = -1.13$  V, which is very similar to that of  $[\text{FeFe}](\text{dcbdt})(\text{CO})_6$  in solution. The larger peak separation and peak broadening is not unexpected and is attributed to slow electron transfer kinetics. Importantly, neither blank FTO nor SAM-FTO electrodes when pre-treated under PSE conditions display any voltammetric features that could be assigned to the  $\text{Fe}_2$  complex (Figure S11). This clearly demonstrates that the observed reduction is a result of  $\text{Fe}_2(\text{dcbdt})(\text{CO})_6$  that is incorporated in the MOF particles close to the electrode surface. CVs of thicker UiO-66-[FeFe](dcbdt)(CO)<sub>6</sub> films show no detectable electrochemical response that could be assigned to the  $\text{Fe}_2$  complex, even though PSE has been evidenced in both films as described above. These electrochemical results suggest that only a negligible amount of  $\text{Fe}_2(\text{dcbdt})(\text{CO})_6$  is present close to the FTO surface in the 20 μm films.

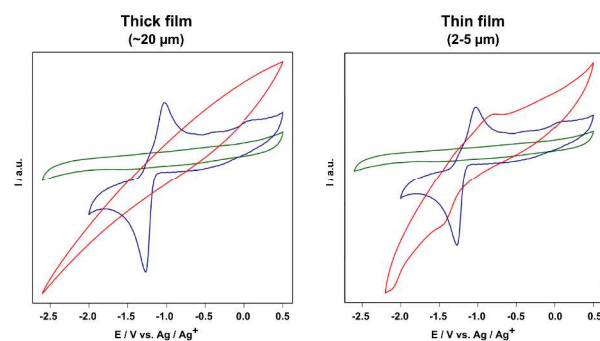


**Fig. 5** Left: Cyclic voltammogram of  $\text{Fe}_2(\text{dcbdt})(\text{CO})_6$  in 1mM DMF solution (blue), and UiO-66 thick film before (green) and after PSE (red). Left: thick UiO-66 film. Right: thin UiO-66 film. All CVs recorded in DMF with 0.1M TBAPF<sub>6</sub> as supporting electrolyte.

In conclusion, we have discovered a solvothermal growth of uniform, crack-free UiO-66 films with high crystallinity and robustness. The film thickness can be tuned by varying the ratio between  $\text{ZrCl}_4$  and  $\text{H}_2\text{bdc}$  that is added during synthesis. Two distinct functional groups, which cannot be directly incorporated using conventional MOF film growth approaches, were incorporated into the film with high efficiency under mild reaction conditions. Electrochemical analysis showed that 20  $\mu\text{m}$  thick UiO-66- $[\text{FeFe}](\text{dcbdt})(\text{CO})_6$  films are not electrochemically active, but in thinner 2-5  $\mu\text{m}$  films, the  $\text{Fe}_2$  complex shows a comparable electrochemical response as the free complex in solution. The strong adhesion of the MOF films and robust nature of UiO-66 provides a versatile platform to synthesize a variety of functional, solid-state thin film materials.

This work was supported by grants from the National Science Foundation, Division of Materials Research (DMR-1262226, H.F., S.M.C.), the Swedish Research Council, Knut and Alice Wallenberg Foundation, and the Swedish Energy Agency (S.P., A.W., S.O.).

## Notes and references

<sup>a</sup>Department of Chemistry and Biochemistry, University of California, San Diego, La Jolla, CA, United States 92093. Tel: 1-858-822-5596; E-mail: scohen@ucsd.edu.

<sup>b</sup>Department of Chemistry, Angstrom Laboratories, Uppsala University, Box 523, 751 20 Uppsala, Sweden. Tel: 46-18-471 7340; E-mail: sascha.ott@kemi.uu.se.

† Experimental details and additional characterization of MOF films. This material is available free of charge via the Internet at <http://pubs.acs.org>.

- (1) O'Keeffe, M.; Yaghi, O. M. *Chem. Rev.* **2012**, *112*, 675.
- (2) Sumida, K.; Rogow, D. L.; Mason, J. A.; McDonald, T. M.; Bloch, E. D.; Herm, Z. R.; Bae, T.-H.; Long, J. R. *Chem. Rev.* **2012**, *112*, 724.
- (3) Suh, M. P.; Park, K. S.; Prasad, T. K.; Lim, D. *Chem. Rev.* **2012**, *112*, 782.
- (4) Yoon, M.; Srirambalaji, R.; Kim, K. *Chem. Rev.* **2012**, *112*, 1196.
- (5) Kreno, L. E.; Leong, K.; Farha, O. K.; Allendorf, M.; Van Duyne, R. P.; Hupp, J. T. *Chem. Rev.* **2012**, *112*, 1105.
- (6) Li, J.-R.; Sculley, J.; Zhou, H.-C. *Chem. Rev.* **2012**, *112*, 869.
- (7) Betard, A.; Fischer, R. A. *Chem. Rev.* **2012**, *112*, 1055.
- (8) Falcaro, P.; Ricco, R.; Doherty, C. M.; Liang, K.; Hill, A. J.; Styles, M. J. *Chem. Soc. Rev.* **2014**, *43*, 5513.
- (9) Stavila, V.; Talin, A. A.; Allendorf, M. D. *Chem. Soc. Rev.* **2014**, *43*, 5994.
- (10) Low, J. J.; Benin, A. I.; Jakubczak, P.; Abrahamian, J. F.; Faheem, S. A.; Willis, R. R. *J. Am. Chem. Soc.* **2009**, *131*, 15834.
- (11) Hu, Y.; Dong, X.; Nan, J.; Jin, W.; Ren, X.; Xu, N.; Lee, Y. M. *Chem. Commun.* **2010**, *47*, 737.
- (12) Demessence, A.; Horcajada, P.; Serre, C.; Boissiere, C.; Grosso, D.; Sanchez, C.; Ferey, G. *Chem. Commun.* **2009**, *101*, 7149.
- (13) Zacher, D.; Shekhah, O.; Woll, C.; Fischer, R. A. *Chem. Soc. Rev.* **2009**, *38*, 1418.
- (14) Shekhah, O.; Liu, J.; Fischer, R. A.; Woll, C. *Chem. Soc. Rev.* **2011**, *40*, 1081.

- (15) Deng, H.; Doonan, C. J.; Furukawa, H.; Ferreira, R. B.; Towne, J.; Knobler, C. B.; Wang, B.; Yaghi, O. M. *Science* **2010**, *327*, 846.
- (16) Cohen, S. M. *Chem. Rev.* **2012**, *112*, 970.
- (17) Deria, P.; Mondloch, J. E.; Karagiari, O.; Bury, W.; Hupp, J. T.; Farha, O. K. *Chem. Soc. Rev.* **2014**, *43*, 5896.
- (18) Brozek, C. K.; Dinca, M. *Chem. Soc. Rev.* **2014**, *43*, 5456.
- (19) Gadzikwa, T.; Lu, G.; Stern, C. L.; Wilson, S. R.; Hupp, J. T.; Nguyen, S. T. *Chem. Commun.* **2008**, 5493.
- (20) Kondo, M.; Furukawa, S.; Hirai, K.; Kitagawa, S. *Angew. Chem., Int. Ed.* **2010**, *49*, 5327.
- (21) Liu, B.; Ma, M.; Zacher, D.; Betard, A.; Yussenko, K.; Metzler-Nolte, N.; Woll, C.; Fischer, R. A. *J. Am. Chem. Soc.* **2011**, *133*, 1734.
- (22) Wang, Z.; Liu, J.; Arslan, H. K.; Grosjean, S.; Hagendorf, T.; Gliemann, H.; Brase, S.; Woll, C. *Langmuir* **2013**, *29*, 15958.
- (23) Wade, C. R.; Li, M.; Dinca, M. *Angew. Chem., Int. Ed.* **2013**, *125*, 13619.
- (24) Kung, C.-W.; Wang, T. C.; Mondloch, J. E.; Fairen-Jimenez, D.; Gardner, D. M.; Bury, W.; Klingsporn, J. M.; Barnes, J. C.; Van Duyne, R.; Stoddard, J. F.; Wasielewski, M. R.; Farha, O. K.; Hupp, J. T. *Chem. Mater.* **2013**, *25*, 5012.
- (25) Maza, W. A.; Ahrenholtz, S. R.; Epley, C. C.; Day, C. S.; Morris, A. J. *J. Phys. Chem. C* **2014**, *118*, 14200.
- (26) Karagiari, O.; Bury, W.; Mondloch, J. E.; Hupp, J. T.; Farha, O. K. *Angew. Chem., Int. Ed.* **2014**, *53*, 4530.
- (27) Fei, H.; Shin, J.; Meng, Y. S.; Adelhardt, M.; Sutter, J.; Meyer, K.; Cohen, S. M. *J. Am. Chem. Soc.* **2014**, *136*, 4965.
- (28) Pullen, S.; Fei, H.; Orthaber, A.; Cohen, S. M.; Ott, S. *J. Am. Chem. Soc.* **2013**, *135*, 16997.
- (29) Streich, D.; Karnahl, M.; Astuti, Y.; Cady, C. W.; Hammarström, L.; Lomoth, R.; Ott, S. *Eur. J. Inorg. Chem.* **2011**, 1106.